The thermal activation of propyl groups on Pt(111)

Demetrius Chrysostomou, Christopher French and Francisco Zaera *

Department of Chemistry, University of California, Riverside, CA 92521, USA

Received 6 July 2000; accepted 7 September 2000

The thermal chemistry of 1- and 2-propyl moieties on Pt(111) was studied by using temperature-programmed desorption (TPD) and reflection–absorption infrared spectroscopy (RAIRS). The propyl intermediates were prepared via thermal activation of the C–I bond of 1- and 2-iodopropane adsorbed precursors, respectively. It was determined that the subsequent thermal activation of those propyl groups results in a competition between reductive elimination to propane, β-hydride elimination to propene, and complete decomposition to propylidyne (and eventually to hydrogen and surface carbon). It was found that while the 2-propyl intermediate favors propene production, 1-propyl also yields significant amounts of propane. The formation of propene via β-hydride elimination was identified by isotopic labeling TPD experiments, and directly about 200 K by RAIRS. Coadsorption experiments with hydrogen and deuterium were used to characterize hydrogenation and H–D reactions. All possible propene and propane isotopomers are formed from both 1- or 2-iodopropane on the D/Pt(111) surface, indicating that exchange is likely to occur via a cyclic propyl–propene–propyl mechanism involving the formation of both 1- and 2-propyl intermediates. Relative rates for 1- versus 2-propyl conversion were estimated.

Keywords: propyl, propene, propane, platinum, H–D exchange, hydrogenation, thermal desorption, infrared spectroscopy

1. Introduction

Many hydrocarbon conversion processes involve alkyl surface intermediates [1,2]. In particular, the first and rate-limiting step in catalytic reforming is believed to be the activation of C–H bonds in alkanes to yield surface alkyl groups. Even though the downstream reactions once those intermediates are formed are quite facile, the relative rates of the different pathways available at that point are what determine the selectivity of the overall processes. This puts the understanding of the reactivity of alkyl moieties on metal surfaces at the center of designing many industrial catalytic systems.

In this work we report on the thermal chemistry of 1- and 2-propyl intermediates on Pt(111) as part of an in-depth investigation undertaken in our laboratory on the thermal chemistry of C_3 alkyl intermediates on Pt(111). Those alkyl groups were prepared via the adsorption and thermal activation of 1- and 2-iodopropane precursors, following an idea from previous studies [3–6]. Propyl intermediates were shown to be an integral part of the thermal hydrogenation of propene, allyl, and metallacycloalkyl moieties to propane on Pt(111) [7–10], and also key intermediates in the extensive H–D exchange observed in the propene and propane temperature-programmed desorption (TPD) data from a number of C_3 intermediates when coadsorbed with deuterium on Pt(111) [7,8]. The formation of propene-d_6 and propane-d_8 desorption products in particular disproves any exchange mechanism which relies solely on allylic intermediates, and argues for a cyclic propene–propyl–propene mechanism instead [8].

Previous investigations into the interaction of alkyl intermediates with transition metal surface provide a framework for the study of the propyl/Pt(111) system. Typically, there are four thermal reaction pathways open to alkyl moieties: reductive elimination with coadsorbed hydrogen to alkanes, β-hydride elimination to alkenes, C–C coupling to another alkane with twice the number of carbons, and decomposition to other surface species (and ultimately to hydrogen and surface carbon). 1-propyl groups on Cu(111) [11,12], Cu(110) [13,14], Al(100) [15], Ni(100) [6], Pt(111) [16], and Au(111) [17] all undergo β-hydride elimination to propene. Propyl adsorbates also incorporate the neighboring surface hydrogen made available through this process to reductively eliminate as propane in all those cases. On the other hand, production of n-hexane by C–C coupling of 1-propyl adsorbates has only been seen on Cu(110) [14], Ag(111) [18], and Au(111) [19]. In terms of the reactivity of 2-propyl groups, this has been studied previously on Ni(100) [20,21] and Rh(111) [22,23] surfaces. While on Rh(111) the main conversion pathway is the production of hydrogen (from total decomposition), significant amounts of propene and propane are produced on Ni(100) as well. Neither Rh(111) nor Ni(100) favor C–C coupling.

In the work discussed here, the thermal chemistry of 1- and 2-propyl intermediates on Pt(111) was investigated by using TPD and RAIRS. It was found that the thermal activation of either propyl group on clean Pt(111) mainly results in β-hydride elimination to propene. Spectroscopic evidence was in fact obtained for the formation of a di-σ-bonded propene surface moiety. In addition, propyl reductive elimination with hydrogen released during the formation of propene leads to the production of some propane.

* To whom correspondence should be addressed.

When comparing the relative rates of β-hydride and reductive elimination for both types of propyl intermediates, it becomes clear that the 2-propyl intermediate favors propene production but the 1-propyl favors propane production instead. The propene formed via β-hydride elimination can also rehydrogenate back to propyl on the surface, to both 1- and 2-propyl species (the former being produced at twice the rate as the latter). This cyclic propyl–propene–propyl reaction involving the formation of both propyl intermediates provides a means for extensive H–D exchange on the adsorbed species when propene, iodopropane, allyl iodide, or other C_3 species are coadsorbed on Pt(111) with deuterium.

2. Experimental

The temperature-programmed desorption (TPD) and reflection–absorption infrared spectroscopy (RAIRS) experiments reported here were performed in a UHV chamber turbo-pumped to a base pressure of 2×10^{-10} Torr described in detail elsewhere [7,24]. For the TPD experiments, this chamber is equipped with a quadrupole mass spectrometer retrofitted with an extendable nose cone. The cone is terminated in a 5 mm diameter aperture, which can be placed within 1 mm of the front face of the single crystal for the selective detection of molecules desorbing from its front surface. The mass quadrupole is interfaced to a personal computer capable of monitoring the time evolution of up to 15 different masses in a single TPD experiment. The TPD data presented here were recorded using heating rates of 5 K/s unless otherwise indicated, and are reported in arbitrary units with relative scales for comparison. A bias of -100 V was placed on the crystal during all TPD experiments to avoid any chemistry induced by the ionizing electrons of the mass spectrometer.

The RAIRS experiments were performed with a Bruker, Equinox 55 FTIR spectrometer. In our set-up, the infrared beam is focused at a grazing incidence ($\sim$85°) through a NaCl window onto the platinum crystal. The reflected light is then passed through a polarizer prior to refocusing onto a narrow-band mercury–cadmium-telluride (MCT) detector [7,25]. The entire beam path is purged with a Balston 75-60 air scrubber in order to remove CO_2 and water from the gas in the path of the beam. All spectra were taken at 4 cm^{-1} resolution, averaging over 4000 scans (which requires approximately 5 min), and were ratioed against spectra of the clean surface taken immediately beforehand. The sample integrity and beam alignment were routinely checked by reproducing published infrared spectra for saturation coverages of CO.

The platinum single crystal was cut in the (111) orientation and polished to a mirror finish using standard procedures, and mounted via two bridging tantalum wires to a sample holder capable of cooling with liquid nitrogen and heating resistively to any temperature between 90 and 1200 K, as monitored by a chromel–alumel thermocouple spot-welded to the edge of the crystal. The sample was cleaned between experiments by treatments at 700 K in 3×10^{-7} Torr O_2 for 3 min to remove any residual carbon, and was deemed clean when the oxygen TPD from saturation with O_2 reproduced those reported in the literature (this O_2 TPD is highly sensitive to residual carbon) [26]. Ar^+ ion sputtering was used sparingly to avoid the creation of surface defects.

1- and 2-iodopropane (>98% purity) were obtained from Aldrich Chemical Company. The liquids were purified by a series of freeze–pump–thaw cycles, and checked by using the chamber's mass spectrometer. Oxygen (>99.9%), CO (>99.9%), and D_2 (>99.5% atom purity) were purchased from Matheson, and used without further purification. Hydrogen (>99.995% pure) was acquired from Liquid Air Products. All exposures are reported in Langmuir (1 L $= 1\times10^{-6}$ Torr s) units, not corrected for ion gauge sensitivities.

3. Results

3.1. TPD survey

We first compare the thermal chemistry of 1- and 2-iodopropane on the Pt(111) surface. Figure 1 shows the TPD spectra obtained from 5.0 L of 1-iodopropane (left panel) and 5.0 L of 2-iodopropane (right panel) adsorbed at 95 K. Shown are the raw desorption traces for 2 (hydrogen), 41 (propene, iodopropane and propane), 29 (propane), and 43 (iodopropane and propane) amu. Since the initial thermal activation of both iodopropanes is expected to yield propyl (either normal or isopropyl) surface intermediates, the chemistry induced by their subsequent thermal activation is expected to be somewhat similar, and this is indeed the case. The desorption data for 1-iodopropane reproduces nicely those reported in the literature [16].

In terms of hydrogen desorption, several peaks are seen in both TPD traces between 240 and 460 K. The onset of hydrogen desorption is less abrupt in the 2-iodopropane case, where the spectrum displays a broader and less structured peak than that from 1-iodopropane. Moreover, the onset temperature is lower with 2-iodopropane, suggesting that alkyl decomposition starts earlier in that case. It is also interesting to note that the hydrogen desorption yield above 380 K is approximately 2.5 times higher for 1-iodopropane than for 2-iodopropane. Hydrogen desorption above 380 K from the thermal activation of C_3 alkyl groups on Pt(111) has generally been associated with the decomposition of propylidyne [7,8,10,16,27], so it is concluded that 2-iodopropane is less adept at forming propylidyne than 1-iodopropane on Pt(111). More on this later.

In order to better highlight the chemistry of the three (propene, propane, and iodopropane) hydrocarbons that desorb in these experiments, the raw data in figure 1 were deconvoluted by following a protocol well established in our laboratory [8,28,29]; the results of this are presented in

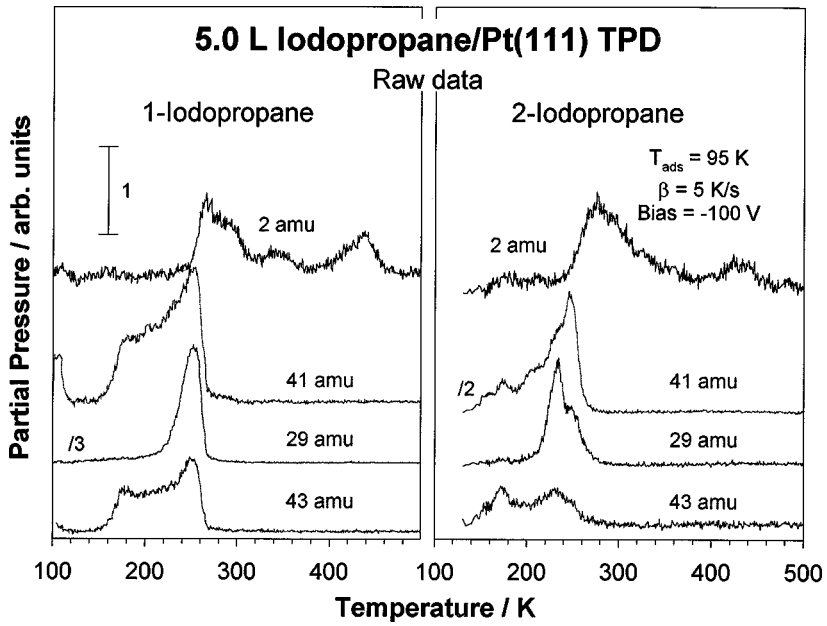

Figure 1. Raw temperature-programmed desorption (TPD) traces for 2, 29, 41, and 43 amu from 5.0 L of 1- (left) and 2-iodopropanes (right) adsorbed on clean Pt(111) at 95 K. The platinum crystal was biased with $V = -100$ V to avoid any radiation-induced chemistry from stray electrons, and a linear heating rate of 5 K/s was used.

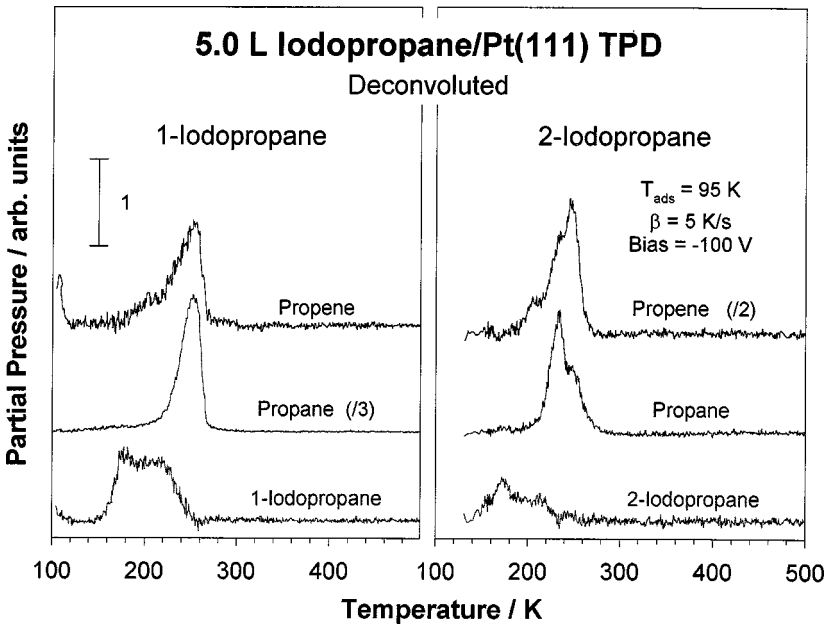

Figure 2. Propene, propane, and molecular desorption traces obtained by deconvolution of the data in figure 1.

figure 2. It is clear in both figures that molecular desorption (43 amu) of both 1- and 2-iodopropane from Pt(111) takes place in two stages, at 170 and 220 K; these are identified with desorption from the multilayer and submonolayer, respectively. Desorption of propene and propane were followed by the signals for 41 and 29 amu, respectively, since those are the ion fragments that show the least overlap [8,28], but the raw traces were also deconvoluted for clarity. In the case of 1-iodopropane, the desorption of both products appears as similar broad features about 250 K, although the propene trace also displays a low-temperature shoulder not matched by that of the saturated hydrocarbon [16]. With 2-iodopropane, however, the spectra for propene and propane both show at least two main desorption features, at 225 and 245 K, and they do not resemble each other as much as in the 1-iodopropane case. Comparing both panels of figure 2, it becomes clear that significantly more propene desorption is seen from 2-iodopropane than from 1-iodopropane. On the other hand, the carbon balance is somewhat maintained because of the corresponding reduction in propane yield. The propene/propane desorption yield ratio was estimated from these data to be

approximately 1 : 2 for 1-iodopropane and 2.5 : 1 for 2-iodopropane (after normalizing for relative mass spectrometer sensitivities).

The regioselectivity of the first dehydrogenation step in propyl moieties adsorbed on Pt(111) was probed by selective deuterium substitution in the iodopropane precursor. Figure 3 presents the results from a TPD experiment with 2-iodopropane-*1,1,1,3,3,3-d*$_6$. Shown are the traces recorded for 2 (H_2), 4 (D_2), and 42 (propene + molecular desorption) amu after a 5.0 L CD_3CHICD_3 dose on Pt(111) at 95 K. These results reveal no H_2 but significant D_2 desorption at 250 K, implying that during the dehydrogenation step to propene deuterium is removed selectively from the β position. Notice also that most of the propene that desorbs molecularly does so before any hydrogen or deuterium evolution. The carbon-containing species left on the surface after heating above 260 K decompose completely into atomic carbon and hydrogen on the surface, and that leads to the desorption of both D_2 around 300, 360, and 460 K and a small but detectable amount of H_2 (2 amu) at 440 K.

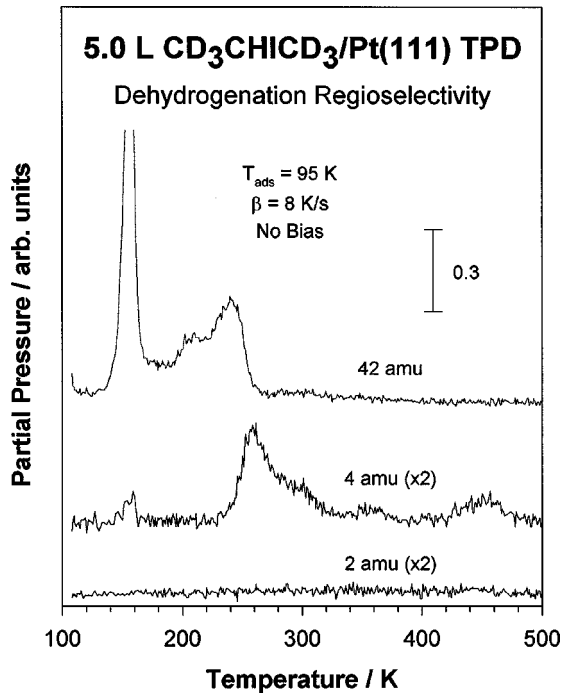

Figure 3. 2 (H_2), 4 (D_2), and 42 (propene) TPD traces from 5.0 L of 2-iodopropane-*1,1,1,3,3,3-d*$_6$ adsorbed on Pt(111) at 95 K. The absence of any significant signal in the 2 amu trace between 250 and 350 K points to the selective nature of the first dehydrogenation step from the β position.

3.2. Hydrogen and deuterium coadsorption

A better insight into the reductive elimination of propyl and isopropyl intermediates on Pt(111) was obtained by preadsorbing hydrogen on the surface. Figure 4 shows the TPD spectra obtained for the cases of 5.0 L of 1-iodopropane (left panel) and 5.0 L of 2-iodopropane (right panel) dosed on Pt(111) surfaces previously exposed to 20 L of hydrogen. Again, the raw data were deconvoluted for the purpose of better following the chemistry of each desorbing species. Most noticeable from these data is the appearance of a broad new propane desorption feature at 185 K in both propyl cases. The absolute yield of this peak is approximately 1.3 times higher from 1-iodopropane than from 2-iodopropane (considerably more propane is made from 1-iodopropane), but its relative contribution to the total propane yield is higher in the latter case. In fact, there is a marked relative increase in propane yield relative to that from the clean surface with both molecules (even

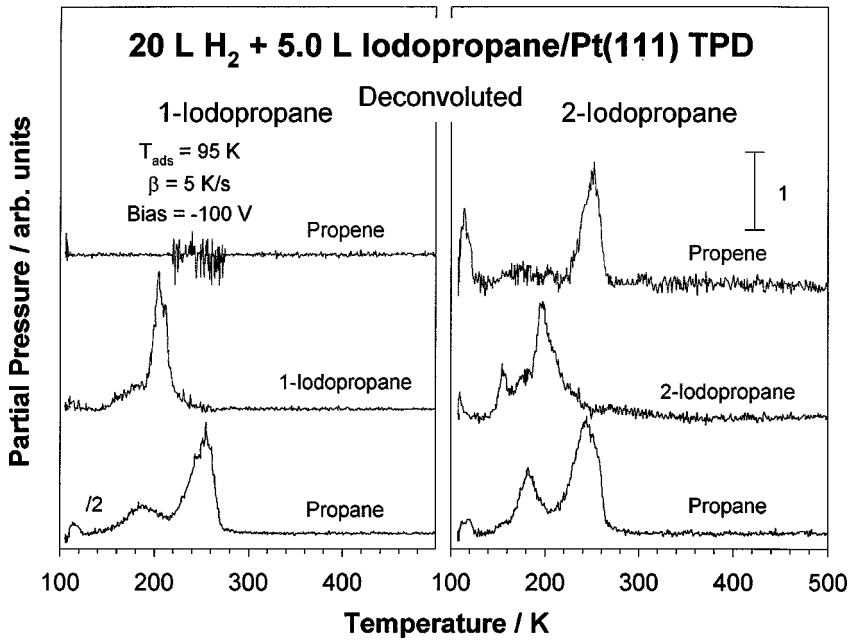

Figure 4. Propene, propane, and molecular desorption traces obtained from deconvolution of raw TPD data for 5.0 L of 1- (left) and 2-iodopropanes (right) adsorbed on Pt(111) predosed with 20 L of H_2.

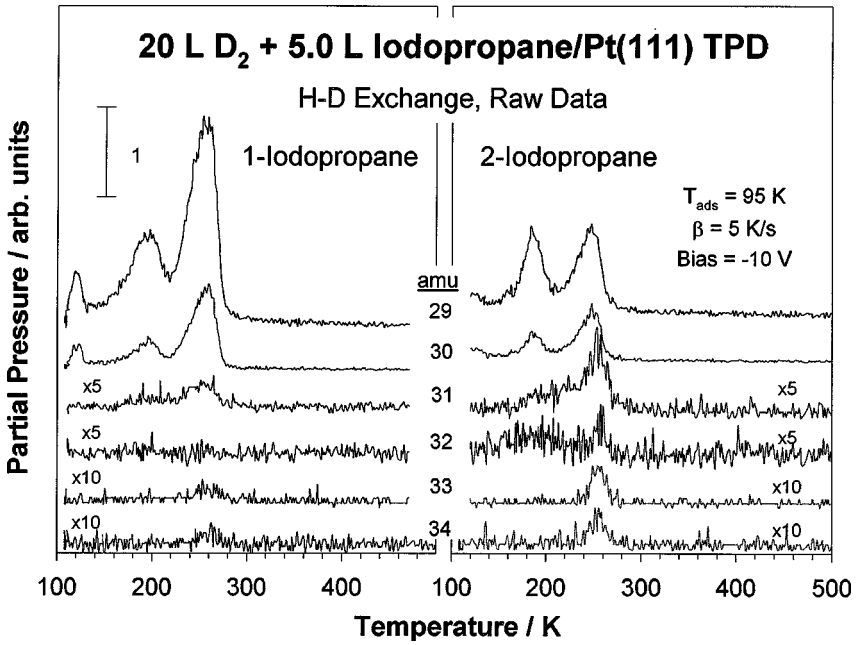

Figure 5. 29, 30, 31, 32, 33, and 34 amu raw TPD traces from 5.0 L of 1- (left) and 2-iodopropanes (right) adsorbed at 95 K on a Pt(111) previously dosed with 20 L of D_2. Multiple H–D exchange is manifested here by the desorption of all possible deuterated propanes, up to propane-d_8.

though the absolute initial iodopropane coverages reached after hydrogen predosing are essentially the same as on clean surfaces). On the other hand, the propene yields are reduced significantly compared to those from the clean surface, particularly in the case of 1-propyl, where the detection of any propene desorption is questionable. Upon hydrogen pretreatment of the surface, the propane/propene desorption yield ratios increase to approximately 2 : 1 for 2-iodopropane and to 1 : ∼0 for 1-iodopropane. No propene desorption is observed below 220 K when hydrogen is present on the surface, and the multiple desorption features seen in the case of 2-iodopropane (for both propene and propane desorption) coalesce into one single peak about 240 K.

The exchange of the hydrogen atoms of the surface intermediates produced by iodopropane activation was characterized via coadsorption experiments with deuterium. Figure 5 shows the TPD spectra resulting from adsorbing 5.0 L of either 1-iodopropane (left panel) or 2-iodopropane (right panel) on Pt(111) pretreated with 20 L of deuterium. The appropriate $C_2D_xH_{5-x}^+$ mass spectrometer fragments from propane were followed by recording the signals in the 29–34 amu range. All fragments up to $C_2D_5^+$ were observed in the 250 K TPD feature for both propyl intermediates, indicating multiple H–D exchange in individual molecules, all the way to propane-d_8 (this was verified with the molecular ion data in the 44–52 amu range). On the other hand, a comparison of the isotopomer yields between the 1- and 2-propyl cases indicates a higher yield of exchanged propanes from the 2-propyl intermediate. This difference is perhaps more noticeable when comparing the desorption signals for propane-d_1 and propane-d_2: the propane-d_1/propane-d_2 yield ratio at 250 K for the 1-propyl moiety is approximately 14 : 1, whereas for 2-propyl it is approximately 6 : 1. There is also a shift to higher temperatures in the peaks corresponding to propanes with more than one deuterium contribution (the 31–34 amu traces), in particular in the case of 2-iodopropane. Finally, in contrast to the behavior seen in the 250 K propane TPD peak, distinguishable signals in the 185 K desorption feature are visible only in the 29 and 30 amu traces, indicating the incorporation of only one deuterium atom in that temperature regime. Clearly, the propane produced at this temperature does not undergo the multiple H–D exchange seen at higher temperatures.

3.3. Infrared characterization

In order to identify the surface intermediates that form during the thermal chemistry of propyl groups on Pt(111), RAIRS data were obtained for both compounds as a function of exposure and surface temperature. The infrared spectra obtained for 10 L of 1- and 2-iodopropane initially adsorbed on Pt(111) at 90 K are shown in figure 6 as a function of annealing temperature (from 90 to 340 K). Each spectrum was acquired at the annealed temperature (unless otherwise indicated), and ratioed against background data recorded under the same conditions.

Exposure of Pt(111) to 10 L of iodopropane at 90 K results in multilayer adsorption (figure 6, bottom spectra). Assignment of the peaks observed in those traces can be easily done by comparison with data from the corresponding liquids [30–33] and from the adsorbed species on Cu(110) [14]. In the case of 1-iodopropane, the symmetric and asymmetric C–H stretching peaks in the terminal methyl group, $\nu_s(CH_3)$ and $\nu_a(CH_3)$, are seen at 2878 and 2970 cm^{-1}, respectively, and the methylene stretch-

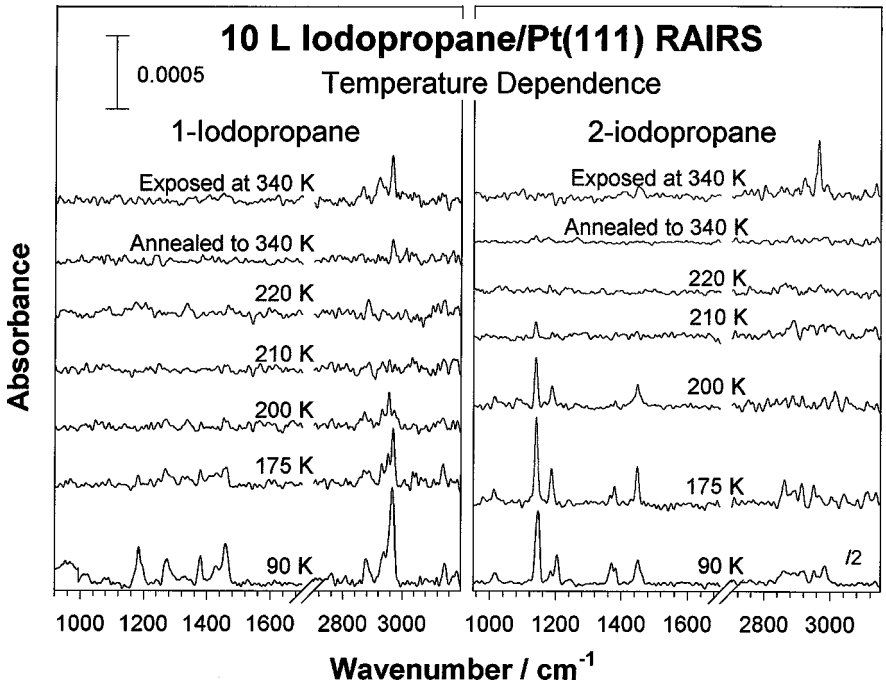

Figure 6. Reflection–absorption infrared spectra (RAIRS) from 5.0 L of 1- (left) and 2-iodopropanes (right) on Pt(111) adsorbed at 95 K and annealed to the indicated temperatures. The top traces correspond to direct adsorption at 340 K. These data point to molecular desorption and to sequential surface propyl, propene, and propylidyne formation.

Table 1
Assignment of the observed vibrational frequencies (in cm^{-1}) in the RAIRS spectra of 1- and 2-iodopropanes adsorbed on Pt(111). The data for the liquid compounds are also provided for reference.

Mode[a]	1-iodopropane	10 L 1-iodopropane/Pt(111)		2-iodopropane	10 L 2-iodopropane/Pt(111)	
	liquid [30–32]	90 K	175 K	liquid [33]	90 K	175 K
$\nu_a(CH_3)$	2967	2970	2970	2983, 2967	2984, 2966	2966
$\nu(CH_2)$	2846, 2938	2941	2955, 2933			
$\nu(CH)$				2951, 2920, 2913	2954, 2916, 2906	2954, 2906
$\nu_s(CH_3)$	2876	2878	2889, 2871	2878, 2861	2894, 2863	2894, 2863
$\delta_a(CH_3)$	1458	1457	1457	1459, 1449	1460, 1450	1450
$\gamma_s(CH_2)$	1435	1428	1428			
$\delta_s(CH_3)$	1380	1377	1377	1383, 1369	1381, 1366	1381, 1366
$\nu(CC) + \delta(CCC)$		1271	1271	1266	1240	1240
$\delta(CHI)$				1201	1202, 1184	1184
$\tau(CH_2)_\beta$, $\omega(CH_2)_\alpha$	1185	1179	1179			
$\nu(CC) + \delta(CCI)$				1141	1140	1140
$\nu(CC)$	1090	1088	1088			
$\rho(CH_3)$				1017	1014	1014

[a] α denotes the CH_2 adjacent to iodine atom, β denotes the CH_2 next to the CH_3 in 1-iodopropane. Nomenclature: ν = stretching, δ = deformation, ρ = rocking, γ = scissoring, τ = twisting, ω = wagging; subindices: s = symmetric, a = asymmetric.

ing, $\nu(CH_2)$, at 2941 cm^{-1}. The corresponding deformation modes are also clearly observed, the symmetric (umbrella) and asymmetric methyl deformation modes, $\delta_s(CH_3)$ and $\delta_a(CH_3)$, at 1377 and 1457 cm^{-1}, respectively, the methylene scissoring, $\gamma(CH_2)$, at 1428 cm^{-1}, the C–C stretching, $\nu(CC)$, at 1088 cm^{-1}, and additional deformations around 1271 and 1179 cm^{-1}. The complete assignment is provided in table 1.

Upon annealing to 175 K, the iodopropane multilayers desorb, and a saturated monolayer is left behind. In the case of 1-iodopropane, annealing to 175 K leads to relative intensity reductions in the CH_2 wagging, $\omega(CH_2)$, and CH_3 asymmetric stretching, $\nu_a(CH_3)$, modes at 1179 and 2970 cm^{-1}, respectively. Further relative reduction of both those peaks continues upon annealing to 200 K, at which point the most dominant features in the spectrum are those at 2960, 2930, and 2880 cm^{-1}. No clear absorbances are identifiable after annealing to 210 K, but a few weak bands reappear at 220 K (see below). Further annealing to 340 K shows the development of a peak at 2965 cm^{-1} corresponding to the asymmetric CH_3 stretching of propylidyne [7].

The assignment of the peaks in the infrared spectra from the multilayer of 2-iodopropane on Pt(111) goes as follows: symmetric and asymmetric methyl C–H stretching peaks, $\nu_s(CH_3)$ and $\nu_a(CH_3)$, at 2863, 2894 and 2966, 2984 cm^{-1}, respectively, α-C–H stretching, ν(CH), at 2954, 2916, and 2906 cm^{-1}, symmetric (umbrella) and asymmetric methyl deformation modes, $\delta_s(CH_3)$ and $\delta_a(CH_3)$, at 1366, 1381 and 1450, 1460 cm^{-1}, respectively, I–C–H deformation, δ(CHI), at 1184 and 1202 cm^{-1}, C–C stretching plus C–C–I deformation combination, $\nu(CC) + \delta(CCI)$, at 1140 cm^{-1}, methyl rocking, $\rho(CH_3)$, at 1014, and an additional deformation around 1240 cm^{-1} [33]. Again, our assignment is summarized in table 1. Annealing to 175 K results in the disappearance of the asymmetric C–H stretching mode, $\nu_a(CH_3)$, at 2984 cm^{-1} (although the spectra in that region are too noisy to make this observation conclusive), and the CHI deformation feature, δ(CHI), at 1202 cm^{-1}. The umbrella $\delta_s(CH_3)$ mode at 1366 cm^{-1} is also reduced with respect to the other $\delta_s(CH_3)$ peak at 1381 cm^{-1}. On the other hand, the band at 1184 cm^{-1} grows, and the strongest rocking mode $\rho(CH_3)$ at 1140 cm^{-1} remains visible up to 210 K. The formation of propylidyne upon annealing the adsorbed 2-iodopropane to 340 K was not detected, but this is not to say that propylidyne does not form in this case, only that its concentration is not high enough to become visible over the experimental noise of the IR data.

The upper spectra in both panels of figure 6 correspond to exposures of Pt(111) to 10 L of 1- and 2-iodopropane directly at 340 K. Peaks at 2965 and 2920 cm^{-1} are clearly seen in both cases, and another feature at 2865 cm^{-1} is apparent in the data from 1-iodopropane. Again, all of those peaks are associated with the formation of propylidyne [7]. By comparing with data from the propene/Pt(111) system [7], the intensities of those peaks are estimated to correspond to propylidyne coverages of about 0.10 ML (in both cases). Notice that the intensities of the features in these spectra are stronger than those obtained by adsorbing the iodopropanes at 90 K and subsequently annealing the surface at 340 K. This is so because in the latter case some of the initial iodopropane desorbs as either propene or propane. Adsorbing at high temperatures allows for the replenishing of the empty sites left by those species. The difference in propylidyne surface coverages between the low- and high-temperature adsorption experiments is more marked for 2-iodopropane. It appears that in the case of 2-propyl surface moieties, propylidyne formation is comparatively slower than propene and propane desorption: while approximately 40% of the 1-propyl moieties end up as propylidyne, less than 15% of 2-propyls do. This may be explained by the change in temperature at which all this chemistry takes place between the two cases: propane desorption starts below 210 K with 2-iodopropane but only above 215 K with 1-iodopropane (see figure 2).

The surface chemistry of the adsorbed propyl groups around 200 K was investigated in more detail with RAIRS.

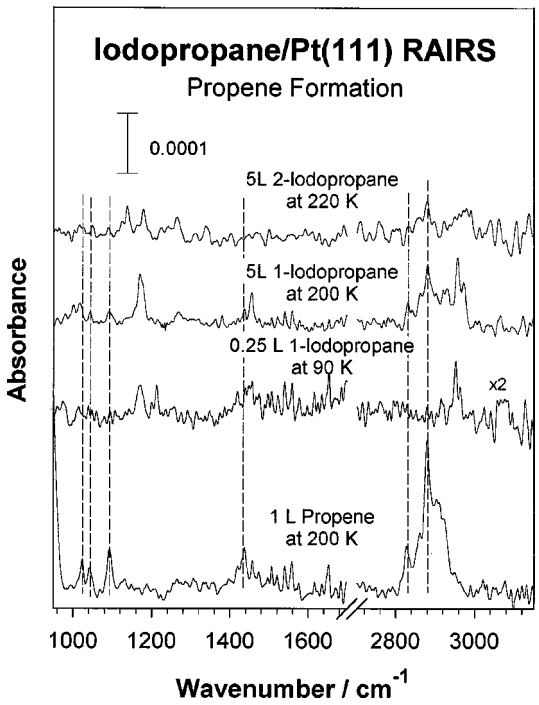

Figure 7. RAIRS evidence for the formation of surface di-σ propene from activation of iodopropanes on Pt(111). The two bottom traces correspond to adsorption of 1.0 L of propene on clean Pt(111) at 200 K and 0.25 L dose of 1-iodopropane at 90 K, and are provided here for reference. The two top traces correspond to 5.0 L of 1- and 2-iodopropane, dosed at 200 and 240 K, respectively. Peaks assignable to propene can be clearly seen in both cases.

Figure 7 offers a comparison among infrared spectra from Pt(111) exposed to 1.0 L of propene at 200 K, 0.25 L of 1-iodopropane at 90 K, 5.0 L of 1-iodopropane at 200 K, and 5.0 L of 2-iodopropane at 220 K. It can be seen there that there are some common features in all those spectra consistent with the formation of di-σ surface propene intermediates. The most prominent peaks in the trace resulting from exposure of the Pt(111) surface to 1.0 L of propene at 200 K are those at 2880 (CH stretch), 2827 (CH_2 symmetric stretch), 1436 (CH_2 scissoring), 1092 (C–CH_3 stretch), 1042 (CH_2 twisting), and 1023 (CH_3 rocking) cm^{-1} corresponding to di-σ-bound propene [7]. All of those features are also evident in the spectrum from 5.0 L of 1-iodopropane adsorbed at 200 K (the extra peaks in that trace are coincident with those for 0.25 L 1-iodopropane at 90 K, and are consequently assigned to a propyl surface entity). Exposure of Pt(111) to 2-iodopropane at 200 K does not show any of the infrared bands of surface propene, but dosing at 220 K does lead to the development of a clear peak at 2880 cm^{-1} and a few small (noisy but reproducible) features at 1090, 1045, and 1020 cm^{-1} in the IR spectrum.

4. Discussion

The results from the study of the thermal conversion of 1- and 2-iodopropane on Pt(111) reported here are consis-

tent with what is known about the surface chemistry of alkyl halides on transition metals. For one, it has been repeatedly reported that, thanks to the lability of the carbon–halide bonds, alkyl halides are good precursors for the preparation of alkyl surface groups [3,5,34]. The carbon–iodine bond in particular is quite weak, and can be broken on metal surfaces around 160–180 K [11,35,36]. The alkyl groups resulting from this activation have been directly identified in a number of cases [14,37,38].

Spectroscopic detection of the onset temperature for the C–I bond scission upon thermal activation of iodopropanes on Pt(111) is still lacking. There is, however, some evidence in our infrared data for the scission of this bond by 175 K. In particular, a relative reduction in the δ(CCI) mode in the case of 2-iodopropane at 1140 cm^{-1} with increasing temperature is accompanied by the disappearance of the δ(CHI) mode at 1202 cm^{-1}. Also, based on the surface dipole selection rule that applies on metal surfaces [38–40], the large intensity reduction in the $\delta_s(CH_3)$ features at 1366 and 1381 cm^{-1} by 200 K argues for the confinement of the methyl groups to a configuration close to parallel to the surface. This would be consistent with an isopropyl group standing up on the surface. There also appear to be slight shifts in frequency in the 1381 and 1141 cm^{-1} peaks when going from 90 to 175 K. In the case of 1-iodopropane, the disappearance of the $\nu_a(CH_3)$ mode at 2984 cm^{-1} suggests a terminal group perpendicular to the surface by 175 K, again what is expected from vertical 1-propyl groups [38]. We propose that the C–I bond in iodopropanes adsorbed on Pt(111) is broken by 175 K, and that that step results in the formation of surface propyl groups.

Heating the surface further leads to the elimination of a hydrogen atom from the beta position from those surface alkyl groups. Past evidence for this β-hydride elimination step has come from a number of observations [3–5,20]. The regioselectivity of this step was first demonstrated with hydrogen (deuterium) TPD data from ethyl iodide on Pt(111) [41]. More direct proof was later added by the detection of the corresponding desorbing alkenes [4,5,20], and production of monodeuterated propene from 1-iodopropane-*2,2*-d_2 on Ni(100) further confirmed the selective removal of the first hydrogen from the beta position [6]. Nevertheless, we believe that here we report the first direct detection of the adsorbed alkene (di-σ-bonded propene) that forms on the surface. Notice in particular the spectra reported in figure 7, where up to six of the modes characteristic of di-σ-bonded propene were observed in the case of 5.0 L of 1-iodopropane adsorbed on Pt(111) at 200 K. Less obvious but still convincing proof for the formation of the same adsorbed olefin from 2-iodopropane is given in the upper trace of that figure. Notice that propene detection from 2-iodopropane was possible only after adsorption at 220 K, not at 200 K as in the case of 1-iodopropane, and that the yield in that case was significantly lower.

The other major contribution from the work reported here is that it provides data for the estimation of the relative rates of hydrogenation and dehydrogenation steps

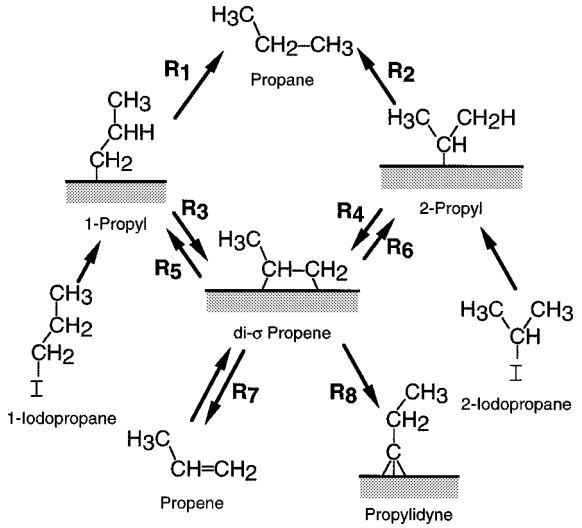

Scheme 1. Mechanism for the hydrogenation and dehydrogenation of propyl moieties on Pt(111).

in 1- and 2-propyl surface moieties. This can be accomplished in large part by analyzing the data from the deuterium coadsorption experiments. It was seen here that the coadsorption of either 1- or 2-iodopropane with deuterium results in extensive H–D exchange. This is not surprising, since propyl groups first dehydrogenate to surface propene, and chemisorbed propene has already been shown to undergo multiple isotopic exchange on Pt(111) [8]. In fact, all propene and propane isotopomers, up to propene-d_6 and propane-d_8, were detected in deuterium coadsorption TPD experiments with either propene or 1- or 2-iodopropane, suggesting that a mechanism involving a cyclic propyl–propene–propyl interconversion is operative in those systems. Clearly, the mechanism responsible for the exchange in the propene and propane that desorb from Pt(111) around 250 K is the same regardless of whether the reaction starts with propene or a propyl precursor.

The propyl/propene H–D exchange mechanism operative around 250 K in the TPD experiments with either propene or iodopropane is summarized in scheme 1. In there, eight different steps are considered in order to account for the hydrogenation and dehydrogenation reactions relevant to the H–D exchange. Starting from the top, R_1 and R_2 are defined as the rates of reductive elimination of 1-propyl and isopropyl, respectively, with surface hydrogen (deuterium) to propane. Next, the β-hydride elimination from those groups to adsorbed propene display rates given by R_3 and R_4, respectively. The rates for the reverse steps, the half-hydrogenation of propene to 1- and 2-propyl, are given by R_5 and R_6, respectively. Finally, the rates of propene molecular desorption and conversion to propylidyne are denoted by R_7 and R_8, respectively. In the following paragraphs relative values for those parameters are estimated. The final results are summarized in table 2.

One important point that needs to be made before embarking in the comparison of the rates for the steps listed

Table 2
Relative reaction rates (R_i) from scheme 1.

Reaction	1-iodopropane	2-iodopropane
Propyl → propane	$R_1 = 1.3R_2$	$R_2 = 0.8R_1$
Propyl → propene	$R_3 = 0.7R_4$	$R_4 = 1.3R_3$
Propene → propyl	$R_5 = 2R_6$	$R_6 = 0.5R_5$

above is the fact that those can vary widely with the specific conditions under which the reactions are carried out [2,42]. In particular, hydrogenation reactions are bimolecular, and therefore depend strongly on the coverages of both the hydrogenating hydrocarbon moiety and surface hydrogen [43,44]. A number of experiments have demonstrated that hydrogenation and H–D yields are very sensitive not only to average surface coverages but also to the local distribution of adsorbed species on the surface [27,44,45]. Dehydrogenation steps may be unimolecular, but are still controlled by the availability of empty sites for the leaving hydrogen atoms [27,46]. Our calculations can only reflect relative rates under specific circumstances. Nevertheless, this is still a useful exercise to help understand reaction selectivities.

One of the most obvious manifestations of the changes in relative rates induced in the systems studied here by changing reaction conditions is the drastic shift in selectivity towards hydrogenation products upon hydrogen or deuterium coadsorption. In the presence of surface hydrogen, hydrogenation steps are typically faster than dehydrogenation reactions [28,47–52]. In the absence of coadsorbed H or D atoms, on the other hand, the rate-limiting step for olefin and alkyl hydrogenation is a dehydrogenation reaction source of the needed hydrogen. In particular, propyl hydrogenation to propane (R_1 and R_2) appears to be much faster than β-hydride elimination to propene below 200 K, especially in the presence of pre-adsorbed hydrogen. Above 200 K, however, the rates for β-hydride elimination from 1-propyl (R_3) and 2-propyl (R_4) are closer (in fact, higher – see later) to R_1 and R_2.

The 185 K propane TPD peak is assigned to the direct reductive elimination of propyl intermediates with surface hydrogen, before any β-hydride elimination takes place. For one, that peak is only seen when the surface is predosed with H_2 or D_2 (figures 2, 4, and 5). Also, its onset is seen about 150 K, a temperature too low to promote any β-hydride elimination; the first appearance of propene desorption from β-hydride elimination occurs at 220 K. More to the point, surface propene was detected by RAIRS only above 200 K. Finally, only propane-d_0, -d_1, and -d_2 are produced below 200 K in experiments with coadsorbed deuterium (figure 5). Dideuteropropane can be made by propyl dehydrogenation to propene followed by sequential deuterations to propyl-d_1 and propane-d_2; no sign of multiple deuteration (production of propane-d_3 to propane-d_8) is seen in that temperature range.

As discussed above, the evidence that the 185 K propane peak is the result of a direct reductive elimination of propyl intermediates with surface hydrogen is compelling. This peak can therefore be used as a measure of the relative rates for the hydrogenation of 1- versus 2-propyl surface moieties. It was estimated that the yield of this peak is approximately 1.3 times higher for 1-iodopropane than for 2-iodopropane (after normalizing to the total respective yields of propene and propane, which are close in both cases), and this roughly translates in a similar relation between reaction rates, $R_1 \approx 1.3R_2$. It is not unreasonable to suggest that 1-propyl groups are more easily hydrogenated than 2-propyl moieties, since the C–Pt bond is sterically more accessible in the 1-propyl intermediate.

Next, the rates of dehydrogenation for 1- versus 2-iodopropane are compared. On visual inspection of figures 2 and 4, it appears that dehydrogenation is easier from 2-propyl groups than from the 1-propyl counterparts. Indeed, more propene desorption (and at a lower temperature) is detected from the former than from the latter in all cases. In the presence of excess hydrogen, the thermal activation of the 2-propyl intermediate leads to comparable yields of propane and propene, while in the case of the 1-propyl intermediate no propene desorption is detected at all. However, the yields for propene desorption cannot be directly used to estimate relative rates for β-hydride elimination, because a significant fraction of the propene produced by that reaction remains on the surface and decomposes at higher temperatures to form propylidyne. This latter species has indeed been identified by RAIRS, see figure 6. By comparison with RAIRS data from adsorption of propene at 300 K [7], it is estimated that the amount of propylidyne produced by high-temperature adsorption of either 1- or 2-iodopropane is approximately the same, 0.10 ML. The propene that does not desorb in the TPD of 1-iodopropane decomposes on the surface instead.

Back to the estimates of dehydrogenation rates, integration of the peaks under the propane and propene TPD traces in figure 2 in the case of 2-iodopropane leads (after calibrating for differences in mass spectrometer sensitivity) to estimates for the yields of those products of approximately 0.07 and 0.03 ML, respectively. Recall that most of the propene produced from this compound desorbs either as propane or propene, and that only 10–15% (0.01 ML) remains on the surface (figure 6). In the case of 1-iodopropane, about half of the propene produced from low-temperature surface saturation followed by annealing remains on the surface as propylidyne (0.04 ML), while the rest desorbs as propene (0.02 ML) and propane (0.04 ML). Here the ratio in propane yield calculated before is obtained again, $R_1/R_2 \approx 0.04/0.03 \approx 1.3$. In addition, the ratio for propene formation is estimated at $R_3/R_4 \approx (0.04 + 0.02)/(0.01 + 0.07) \approx 0.7$. It is interesting to point out that β-hydride elimination takes place preferentially from internal carbons [53]. It is not entirely clear why propene molecular desorption is easier when starting with 2-iodopropane.

Finally, it is interesting to compare the relative rates of propene hydrogenation to 1- and 2-propyl moieties.

Again, we resort to the use of the H–D exchange data for propene [8] for this. Deuterium exchange can only take place in the center carbon of the 1-propyl group and the end carbons of the 2-propyl group, yet all propane isotopomers are detected in the TPD experiments. This means that it must be possible for the hydrogenation of propene to start at either carbon around the double bond. In other words, hydrogenation of propene to both 1- and 2-propyl intermediates are operative in the propene/Pt(111) system. On the other hand, when D/Pt(111) is exposed to propene, the resulting thermal desorption yields of propene-d_5 and propane-d_7 are lower than those expected for an exponential distribution of exchanged alkyl groups [8]. The facile hydrogenation of the center carbon atom to form 1-propyl intermediates over 2-propyl can explain this observation; the opposite would lead to the early exchange of the end hydrogens and the subsequent desorption of significant amounts of propene-d_5 and propane-d_7. With this information we can predict that R_5 in scheme 1 is faster than R_6. Based on the fact that the propene-d_5 yield in the D + propene/Pt(111) TPD experiments deviates by a factor of 2–5 from an exponential distribution [8], R_5 can be estimated to be at least two times R_6.

Experimental estimates of the propyl hydrogenation-to-dehydrogenation ratios can in principle be made by using the exchange information in figure 5, by using the propane-d_1/propane-d_2 yield ratio from iodopropane activation on deuterium-predosed Pt(111). This is so because incorporation of one deuterium atom prior to propane desorption is associated with the direct conversion of propyl groups to propane via reductive elimination. The incorporation of two D atoms into desorbing propane, on the other hand, is indicative of the amount of propyl that first β-hydride eliminate to propene and then deuterate twice to propane. The propane-d_1/propane-d_2 yield ratios from coadsorption of 1- and 2-propyl intermediates with deuterium are indeed quite different, 14 : 1 and 6 : 1, respectively. This points again to the relative ease with which 1-propyl groups hydrogenate compared to 2-propyl moieties, which tend to dehydrogenate instead. From these data, $R_1/R_3 \approx 2.3(R_2/R_4)$. The estimates obtained in the previous paragraph yield a factor of $\sim$1.9 instead, but this is because the isotopomer ratios only provide an upper limit which does not take into account multiple exchanges of deuterated molecules with surface H atoms.

As mentioned before, comparing hydrogenation versus dehydrogenation rates is particularly difficult because of the dramatic effect that surface coverages exert on those. The data presented here indicate that, at least at saturation, propyl hydrogenation is significantly faster than propyl dehydrogenation. The propane-d_1/propane-d_2 yield ratios in figure 5 suggest that the R_1/R_3 and R_2/R_4 ratios are about 14 and 6, respectively. On the other hand, as the surface coverages decrease (because of the desorption of propane and propene), β-hydride elimination becomes easier, and in fact dominates the overall hydrocarbon conversion, since the overall TPD yields of propene from iodopropanes are between 1.5 (1-propyl) and 2.7 (2-propyl) times higher than those for propane. Also, propyl conversion must be even faster, because at no point in any of the experiments with propene the population of surface propyl reaches detectable levels (propene from propyl, on the other hand, was detected by RAIRS). Lastly, propene hydrogenation to propyl must be relatively fast compared to propene desorption or decomposition to propylidyne, because that is the first step responsible for the extensive H–D exchange observed [8]. All this sets propene hydrogenation to propyl as rate limiting for H–D exchange and for propane production (notice the peak maxima shift seen in the propane TPD spectra as the deuterium content of the molecule increases). In this scenario, the yield of propane is controlled by two competing factors, the rate of propene half-hydrogenation to propyl (the rate-limiting step), and the ratio of propyl hydrogenation to dehydrogenation rates. Also, H–D exchange is facile, and occurs extensively and at low temperatures (direct evidence for this was recently reported for the case of ethylene [44]). Finally, the isotopomer distributions are controlled by the local coverages of atomic hydrogen and deuterium surrounding the propene molecules on the surface.

A kinetic model can be developed from these observations. Quantification of any model, however, is particularly difficult because: (1) this is a "stiff" mechanism, that is, it contains steps with widely different rates, (2) changes in surface coverages affect rates in significant ways (notice, for instance, how only hydrogenation is seen below 200 K on iodopropane-saturated surfaces), and (3) the local distribution of hydrogen and deuterium atoms on the surface and their relative mobility play a key role in determining the deuterium content of the H–D exchanged molecules. A simple isothermal computer integration of the rate laws from our mechanism was performed in order to identify the trends associated with the different rate constants. The following was concluded: (1) propyl + hydrogen reductive elimination has to be at least an order of magnitude faster than propene hydrogenation to propyl in order not to build up a significant propyl population on the surface; (2) propyl β-hydride elimination needs to be at least another order of magnitude faster (a factor of 20–50 faster than propyl hydrogenation) to explain the low propane yields; and (3) some hydrogen coadsorption (from the background) and limited H and D surface mobility is required to limit the extent of the H–D exchange (otherwise an equilibrium distribution of isotopomers would be produced). These represent relative rate estimates for submonolayer coverages.

Finally, it is worth repeating that the relative rates of the steps depicted in scheme 1 depend on the conditions of the experiments considered. This is particularly important when comparing hydrogenation versus dehydrogenation rates. It is clear that an increase in hydrogen coverage tips the selectivity towards the former family of reactions. On the other hand, H_2 usually competes unfavorably with hydrocarbons for surface sites under catalytic

conditions [2]. In any case, a rapid alkane–olefin equilibrium is almost always reached in reforming processes with metal catalysts. What is important is what happens once alkyl intermediates are formed on the surface, because that defines the selectivity of many industrial processes. In that respect, the small differences in conversion rates between 1- and 2-propyl groups estimated here become critical. Only differences of 20–30% were detected in hydrogenation and dehydrogenation steps between those two groups (table 2), but those are enough to define the dominant pathways of many hydrocarbon conversion processes. Also, because these rate ratios are relative, they are reliable (in spite of their closeness to unity), and not expected to vary significantly with coverages.

5. Conclusions

A comparative investigation of the thermal chemistry of 1- and 2-propyl intermediates has led to a greater insight into the mechanisms involved in propene and propane formation from C_3 alkyl intermediates on Pt(111). It was found that thermal activation of propyl groups on that surface results in a competition between β-hydride elimination to propene and reductive elimination with surface hydrogen to propane. In the absence of surface hydrogen, reductive elimination can only take place once reactive hydrogen has been liberated via β-hydride elimination. The formation of propene by β-hydride elimination was identified around 200 K directly by infrared spectroscopy. In that case, 1-propyl moieties yield at least twice as much propane as gas-phase propene, and significant (about half) propylidyne is left on the surface, whereas with 2-propyl moieties the propene-to-propane yield ratio reaches a value above two, and almost no surface decomposition is observed. β-hydride elimination from 2-propyl was estimated to be about 1.3 times faster than from 1-propyl, but only 20% as fast when calculated per available β-hydrogen.

When hydrogen is preadsorbed on the surface, propane yields increase greatly at the expense of propene production. Indeed, in the case of the 1-propyl group, no propene desorption is detected at all. Propane formation is also seen at lower temperatures, below 200 K, indicating that in the case of the clean surface the rate-limiting step is propyl dehydrogenation. Based on the relative yields of propane below 200 K on the H/Pt(111) surface, the rate of 1-propyl hydrogenation was estimated to be about 30% higher than that of 2-propyl.

When coadsorbed with deuterium, both propyl intermediates exhibit extensive deuterium incorporation into the desorbing propenes and propanes. All isotopomers, up to propene-d_6 and propane-d_8, desorb from the surface, indicating a cyclic propyl–propene–propyl reaction involving the formation of both types of propyl intermediates. The 1-propyl moiety is responsible for exchange of the hydrogens on the center carbon atom, while the 2-propyl intermediate is responsible for exchange on the end carbons. Based on the product distributions of the propane and propene isotopomers in deuterium + propene coadsorbed experiments, it was estimated that hydrogenation of the central carbon is at least twice as fast as hydrogenation of the end methylene group.

Acknowledgement

Financial support for this project was provided by the National Science Foundation under Grant No. CHE-9819652.

References

[1] G.C. Bond and P.B. Wells, Adv. Catal. 15 (1964) 91.
[2] F. Zaera, Isr. J. Chem. 38 (1998) 293.
[3] F. Zaera, Acc. Chem. Res. 25 (1992) 260.
[4] F. Zaera, Chem. Rev. 95 (1995) 2651.
[5] B.E. Bent, Chem. Rev. 96 (1996) 1361.
[6] S. Tjandra and F. Zaera, Langmuir 10 (1994) 2640.
[7] F. Zaera and D. Chrysostomou, Surf. Sci. 457 (2000) 71.
[8] F. Zaera and D. Chrysostomou, Surf. Sci. 457 (2000) 89.
[9] D. Chrysostomou and F. Zaera, J. Phys. Chem. B (2000), submitted.
[10] D. Chrysostomou, J.M. Guevremont, A. Chou and F. Zaera, in preparation.
[11] J.-L. Lin and B.E. Bent, J. Phys. Chem. 96 (1992) 8529.
[12] J.G. Forbes and A.J. Gellman, J. Am. Chem. Soc. 115 (1993) 6277.
[13] C.J. Jenks, C.-M. Chiang and B.E. Bent, J. Am. Chem. Soc. 113 (1991) 6308.
[14] C.J. Jenks, B.E. Bent, N. Bernstein and F. Zaera, J. Am. Chem. Soc. 115 (1993) 308.
[15] B.E. Bent, R.G. Nuzzo, B.R. Zegarski and L.H. Dubois, J. Am. Chem. Soc. 113 (1991) 1137.
[16] T.B. Scoggins, H. Ihm and J.M. White, Isr. J. Chem. 38 (1998) 353.
[17] A. Paul, M.X. Yang and B.E. Bent, Surf. Sci. 297 (1993) 327.
[18] X.-L. Zhou and J.M. White, J. Phys. Chem. 95 (1991) 5575.
[19] A.M. Paul and B.E. Bent, J. Catal. 147 (1994) 264.
[20] S. Tjandra and F. Zaera, J. Am. Chem. Soc. 117 (1995) 9749.
[21] N.R. Gleason and F. Zaera, J. Catal. 169 (1997) 365.
[22] C.W.J. Bol and C.M. Friend, J. Phys. Chem. 99 (1995) 11930.
[23] F. Solymosi, J. Mol. Catal. A 131 (1998) 121.
[24] H. Hoffmann, P.R. Griffiths and F. Zaera, Surf. Sci. 262 (1992) 141.
[25] F. Zaera, H. Hoffmann and P.R. Griffiths, Vacuum 41 (1990) 735.
[26] V.P. Zhdanov and B. Kasemo, Surf. Sci. 415 (1998) 403.
[27] F. Zaera, Langmuir 12 (1996) 88.
[28] S. Tjandra and F. Zaera, Surf. Sci. 322 (1995) 140.
[29] F. Zaera and C.R. French, J. Am. Chem. Soc. 121 (1999) 2236.
[30] G.A. Crowder and S. Ali, J. Mol. Struct. 25 (1975) 377.
[31] K. Tanabe and S. Saëki, J. Mol. Struct. 27 (1975) 79.
[32] Y. Ogawa, S. Imazeki, H. Yamaguchi, H. Matsuura, I. Harada and T. Shimanouchi, Bull. Chem. Soc. Jpn. 51 (1978) 748.
[33] P. Klaboe, Spectrochim. Acta A 26 (1970) 87.
[34] F. Zaera, J. Mol. Catal. 86 (1994) 221.
[35] F. Zaera, Surf. Sci. 219 (1989) 453.
[36] S. Tjandra and F. Zaera, J. Vac. Sci. Technol. A 10 (1992) 404.
[37] S. Tjandra and F. Zaera, Surf. Sci. 289 (1993) 255.
[38] C.J. Jenks, B.E. Bent, N. Bernstein and F. Zaera, J. Phys. Chem. B 104 (2000) 3008.
[39] R.G. Greenler, J. Chem. Phys. 44 (1966) 310.
[40] F. Zaera, H. Hoffmann and P.R. Griffiths, J. Electron Spectrosc. Relat. Phenom. 54/55 (1990) 705.
[41] F. Zaera, J. Am. Chem. Soc. 111 (1989) 8744.
[42] M. Xu, J. Liu and F. Zaera, J. Chem. Phys. 104 (1996) 8825.
[43] T.V.W. Janssens and F. Zaera, J. Phys. Chem. 100 (1996) 14118.

[44] T.V.W. Janssens, D. Stone, J.C. Hemminger and F. Zaera, J. Catal. 177 (1998) 284.
[45] F. Zaera, J. Catal. 121 (1990) 318.
[46] T.V.W. Janssens and F. Zaera, Surf. Sci. 344 (1995) 77.
[47] F. Zaera, Surf. Sci. 262 (1992) 335.
[48] S. Tjandra and F. Zaera, J. Catal. 144 (1993) 361.
[49] S. Tjandra and F. Zaera, J. Catal. 147 (1994) 598.
[50] F. Zaera and G.A. Somorjai, J. Am. Chem. Soc. 106 (1984) 2288.
[51] A. Loaiza, M. Xu and F. Zaera, J. Catal. 159 (1996) 127.
[52] F. Zaera, J. Phys. Chem. 94 (1990) 5090.
[53] C.J. Jenks, B.E. Bent and F. Zaera, J. Phys. Chem. B 104 (2000) 3017.